SUPPORTING INFORMATION

SUPPLEMENTARY METHODS

Gut tissue dissociation: For isolation of neonatal (P0) and adult (8 weeks) mouse enteric cells, the entire small intestine and/or colorectum were harvested from C57BL/6J mice, and the outer smooth muscle/myenteric plexus layer was separated from the underlying submucosa/epithelium. For isolation of fetal mouse enteric cells, the whole small and/or large intestine was used for dissociation without prior separation of the gut layers. Adult outer smooth muscle/myenteric plexus cells were enzymatically dissociated in two steps, first by treating with 1 mg/ml collagenase IV (Worthington Biochemicals) dissolved in Hank's buffered salt solution (HBSS) containing 0.5 mM $CaCl_2$ and no Mg^{2+} for 30 minutes at 37ºC. After briefly washing with HBSS without calcium and magnesium (HBSS-free) and centrifugation, the partially dissociated tissue was further dissociated with 10 Units/ml papain (Worthington Biochemicals) for 10 minutes at 37ºC without agitation. The enzymatic reaction was terminated by quenching with ice-cold staining medium (L15 medium (Invitrogen) supplemented with 1% penicillin/streptomycin (Invitrogen), 1 mg/ml BSA (Sigma), and 10 mM HEPES pH 7.4 (Invitrogen)) containing 100 Units/ml bovine pancreas DNase I (Sigma). The partially dissociated tissue was then pelleted by centrifugation, resuspended in ice-cold staining medium containing DNase I, mechanically dissociated by gentle trituration and filtered through 40 μm nylon mesh (Sefar) to yield a single cell suspension.

Dissociation of neonatal outer smooth muscle/myenteric plexus layer tissue and fetal guts were performed as previously described (56), using a mixture of 0.25 mg/ml collagenase IV (Worthington Biochemicals) and 0.005% trypsin-EDTA (Invitrogen, 1:10 dilution of a 0.05% stock) in HBSS-free for 20 minutes at 37ºC. The partially dissociated tissues were then pelleted by centrifugation, resuspended in ice cold staining medium containing DNase I, mechanically dissociated by gentle trituration and filtered through 40 μm nylon mesh.

Antibodies and flow-cytometry: A complete list of all primary and secondary antibodies used in this study, and their sources, can be found in Table S1. Live cells were stained with primary and secondary antibodies diluted in staining medium for 30 minutes each on ice. Cells were stained with 2 μg/ml 4',6-diamidino-2-phenylindole (DAPI; Sigma) immediately before flow-cytometry to exclude dead cells. Staining of fixed cells for intracellular antigen expression was performed in PGN for 30 minutes on ice. PGN contained PBS supplemented with 5% goat serum (Invitrogen), 1% BSA, 0.3% Triton X-100 (Sigma) and 0.1% NaN_3 (Sigma). All flow cytometry was performed on a customized FACSAria II three-laser, ten-color flow cytometer (Becton-Dickinson).

To assess CD49b expression on enteric NCSCs at different developmental stages, freshly dissociated fetal, neonatal and/or adult mouse gut cells were stained with FITC conjugated monoclonal hamster-anti-mouse CD49b and APC conjugated monoclonal antibodies against a panel of lineage markers, including the pan-leukocyte marker CD45, the erythroid cell marker TER119, and the pan-endothelial cell marker CD31. Unfractionated, $CD49b^+$, $CD49b^-$, $lineage^+$, $lineage^-$ and $CD49b^+lineage^-$ cells were sorted into 6 or 96-well ultralow binding plates (Corning Incorporated) to assess their ability to form multipotent neurospheres.

For staining of intracellular antigens in $CD49b^+Lineage^-$ cells, freshly isolated adult mouse gut cells were first stained for CD49b and lineage markers as described, washed once with PBS, then fixed with 2% paraformaldehyde (PFA) in PBS for 10 minutes on ice. The fixed gut cells were blocked in PGN for 30 minutes on ice, then stained with antibodies against mouse GFAP, SOX10, S100B, Nestin or HuD. PE-conjugated secondary antibodies (Jackson ImmunoResearch) were used to visualize the primary antibody staining. Isotype control staining was performed in parallel to establish the background threshold.

For cell cycle analysis of adult $CD49b^+Lineage^-$ cells, freshly isolated adult mouse gut cells were first stained with CD49b and lineage markers, then $CD49b^+Lineage^-$ cells were sorted and resorted (to ensure purity) into 70% ethanol and fixed at -20ºC overnight. The cells were

spun down, washed once with PBS, then resuspended in PGN containing 50 µg/ml propidium iodide (PI) and 0.1 mg/ml RNase A before being analyzed for DNA content by flow cytometry. Unfractionated whole bone marrow cells were used as a positive control, which showed approximately 10% cells in the S/G2/M phase of the cell cycle.

Cell culture: Neurospheres were cultured non-adherently in ultra low binding 6 or 96-well plates (Corning Incorporated). NCSC 'self-renewal' medium contained a 5:3 mixture of DMEM-low gluocose (Invitrogen) and Neurobasal (Invitrogen) medium supplemented with 15% chick embryo extract (CEE; prepared as described, (47)), 20 ng/ml recombinant human bFGF (R&D Systems), 20 ng/ml IGF1 (R&D Systems), 1% N2 supplement (Invitrogen), 2% B27 supplement (Invitrogen), 50 µM 2-mercaptoethanol, 35 ng/ml retinoic acid (Sigma), and penicillin/streptomycin (Invitrogen). For clonal density cultures, 2000 unfractionated gut cells or equivalent numbers of flow-cytometrically isolated cells (the number of cells from the relevant cell population that would be contained within 2000 unfractionated cells) were sorted into each well of 6-well plates containing 1.5 ml self-renewal medium. For clonal culture of single cells, individual $CD49b^{+}Lineage^{-}$ cells were sorted into each well of a 96-well plate containing 100 µl of self-renewal medium then the wells were visually inspected to ensure that each well contained a single cell. All cultures were maintained in 6% CO_2/balance air at 37ºC, and neurospheres were counted and/or replated for differentiation after 10 days.

To assess the differentiation of primary neurospheres, individual neurospheres were replated into a 96-well tissue culture plate (Corning) pre-coated with 150 µg/ml poly-d-lysine (Biomedical Technologies) and 0.15 mg/ml human fibronectin (Biomedical Technologies) containing 'differentiation' medium (same as self-renewal medium but containing only 1% CEE, 10 ng/ml FGF and no IGF). Adherent cultures were maintained at 37˚C in 6% CO2/balance air for 7-10 days before fixing and staining for neuronal, glial and myofibroblast markers.

To assess the self-renewal potential of primary neurospheres, individual primary neurospheres were replated (1 per well) into each well of a 48-well tissue culture plate, pre-coated with 0.15 mg/ml fibronectin, and cultured in self-renewal medium for 48 hours to allow the colonies to flatten out. The flattened colonies were then digested with 0.05% trypsin-EDTA followed by quenching with cold staining medium and mechanical dissociation. One thousand of the dissociated cells were plated into each well of 6-well ultra low binding plates and cultured in self-renewal medium for 10 days. At the end of the culture period, secondary neurospheres were counted and replated into adherent culture to allow differentiation and assessment of multilineage differentiation potential as described for primary neurospheres.

Immunohistochemistry on freshly sorted or cultured cells: For staining of differentiated neurospheres, replated neurospheres were fixed in acid ethanol (5% glacial acetic acid in 100% ethanol) for 20 minutes at -20°C, washed, blocked in PGN and triply labeled with antibodies against Peripherin, GFAP and αSMA as described (57). Peripherin staining was visualized using Alexa Fluor 647 conjugated goat-anti-rabbit IgG secondary antibody (Invitrogen). GFAP staining was visualized using Alexa Fluor 555 conjugated goat-anti-mouse IgG_1 (Invitrogen) and αSMA was visualized using Alexa Fluor 488 conjugated goat-anti-mouse IgG_{2a} (Invitrogen). Cell nuclei were counter stained with 2 μg/ml DAPI in PGN.

To assess the plating efficiency of $CD49b^+Lineage^-$ cells, 50 $CD49b^+Lineage^-$ cells were sorted into each well of a 96-well plate pre-coated with 50 ng/ml fibronectin, and cultured for 6-8 hours in self-renewal medium at 37°C. The number of remaining cells after overnight culture was counted after fixation in acid ethanol and DAPI staining. Plating efficiency was calculated as the number of cells that survived the initial culture period divided by the number of cells sorted into culture. For GFAP staining of freshly sorted $CD49b^+Lineage^-$ cells, 50-100 $CD49b^+Lineage^-$

cells were sorted onto a microscope slide, air-dried for 2 hours, then fixed with acid ethanol and stained with DAPI and antibody against GFAP as described above.

Additional gut lesions: For partial stenosis injuries, a loop of non-absorbable suture (Tevdek II, 3-0) was tied around the outside of the gut lumen, without narrowing the intestine. The region proximal to the stitch becomes distended during gut transit and the region with the stitch is unable to distend, resulting in a partial stenosis (58, 59). After the stitch was instated, the ileum was placed back into the abdomen and the midline incision was closed as described above. BrdU treatment was started on the day after surgery and continued for 2 weeks then chased for 2 weeks.

To partially ablate enteric glia, ganciclovir was administered to adult *Gfap-tk* mice using subcutaneously implanted osmotic minipumps (Alzet osmotic pumps; Durect Corporation) for a duration of 1-4 weeks as previously described (51). Ganciclovir was administered at a rate of 100 mg/kg body mass/day for 7 days in some experiments, 50 mg/kg body mass/day for 14 days in some experiments, and 10 mg/kg body mass/day for 28 days in other experiments. BrdU was started on the last day of ganciclovir administration and continued for 10 to 14 days then chased for 10 to 21 days (Table 1).

For gut inflammation studies, 8 week old C57BL/6 mice were treated with dextran sulfate sodium (DSS) (60), Indomethacin (61), *Yersinia pseudotuberculosis* (62) or *Citrobacter rodentium* (63) as previously described. DSS was administered in drinking water (3%) for 7 days, causing peak inflammation in the colon 5-7 days later (60). BrdU was started on the third day of DSS treatment. For Indomethacin treatment, one dose of 25 mg/kg Indomethacin was injected subcutaneously causing peak inflammation in the proximal small intestine and stomach 24 hours post treatment (61). Two mice were injected with 2 doses of 25 mg/kg on consecutive days. BrdU was started on the same day as the first injection. For *Citrobacter rodentium* infection, a single dose of $1x10^9$ bacteria (strain DBS120) was administered orally, causing peak

inflammation in the distal colon 12 days after infection (63). BrdU was started on the third day after infection. For *Yersinia pseudotuberculosis* infection, a single dose of $1x10^9$ bacteria (strain IP2777 yopHR409A, a gift of James Bliska, SUNY Stony Brook) was administered orally, resulting in peak inflammation in the cecum 3-4 days after infection (62). BrdU was started on the second day after infection. In all cases, BrdU treatment was continued for 6 weeks then chased for 2 weeks (Table 1).

For irradiation injury experiments, C57BL/6 mice were lethally irradiated with an Orthovoltage X-ray source delivering approximately 300 rad/minutes in two equal doses of 570 rad, delivered at least 2 hours apart. The mice were then rescued from hematopoietic failure by transplanting 150 Thy-1^{low}Lineage$^{-/low}$Sca-1^{+}c-kit^{+} hematopoietic stem cells (64). BrdU was started on the third day after irradiation and continued for 3 weeks then chased for 2 weeks before the mice were sacrificed for analysis.

Assessing gut neurogenesis under other physiological and pathophysiological conditions: For rats that were administered a high fat, high protein, high carbohydrate, or liquid diet (Purina Mills Test Diet), BrdU was started on the same day as the test diet. Rats received the test diet for 3 weeks and the BrdU for 4 weeks such that BrdU administration was stopped one week after the test diet was stopped. The BrdU was then chased for 1 to 8 months before the rats were sacrificed for analysis.

To test whether voluntary exercise could stimulate adult ENS neurogenesis similar to what was found in the CNS dentate gyrus (18), a running wheel was placed into the cages of 8-week old C57BL/6 mice for 6 months. The mice were housed one mouse per cage. BrdU was started on the same day as the running wheel and continued for 4 months. The mice were then continued on the running wheel and chased for another 2 months before being sacrificed for analysis. Use of the running wheels was confirmed by odometers that found the mice ran 1305 to 1871 kilometers over the six month period. To test whether pregnancy induces gut

neurogenesis, BrdU was administered to pregnant Sprague-Dawley rats at E14.5 and continued for 3 weeks, followed by 4-8 weeks chase. To test whether diabetic neuropathy induces enteric neurogenesis, Sprague-Dawley rats were rendered hyperglycemic by streptozotocin administration to ablate pancreatic β-cells as previously described (49). After hyperglycemia developed, BrdU was administered for 2 weeks, followed by a 2-4 weeks chase without BrdU.

Confocal analysis: All confocal images were collected on a Zeiss LSM 510 (Carl Zeiss) or a Leica TCS SP5 (Leica microsystems) confocal laser-scanning microscope using a 63x/NA1.4 or a 20x/NA0.7 oil immersion objective. 1 µm thick optical sections were scanned through the tissue specimens creating a Z-series stack. Three-dimensional projections were made using LSM 510 or Leica LAS AF lite software. Channel overlay and image assembly was performed in ImageJ and Adobe Photoshop software.

SUPPLEMENTARY FIGURE LEGENDS

Figure S1: The specificity of primary antibody staining. A-G) To confirm the specificity of all primary antibody staining, we stained adjacent gut tissue with appropriate isotype control immunoglobulins, side-by-side with each primary antibody. In all cases, specific staining was observed with the primary antibodies, but not with isotype controls.

Figure S2: Most adult mouse enteric glia express CD49b. A) A representative image of secondary neurospheres derived from a single, multipotent primary neurosphere. All multipotent primary neurospheres were capable of generating secondary neurospheres. On average, each primary neurosphere generated 668±114 multipotent secondary neurospheres. B) Flow-cytometric analysis of fixed adult Lineage$^-$S100B$^+$ and Lineage$^-$GFAP$^+$ gut cells stained with isotype control antibody (open histograms) or anti-CD49b antibody (grey shaded histograms). Most Lineage$^-$S100B$^+$ and Lineage$^-$GFAP$^+$ cells were CD49b$^+$. C-E) Representative whole

mount immunofluorescence staining showing CD49b staining co-localized with p75, GFAP and Nestin staining throughout adult myenteric ganglia, in a pattern consistent with enteric glia.

Figure S3: Neurogenesis was readily detected by BrdU incorporation in the adult dentate gyrus of all rats examined. A) As a positive control for adult neurogenesis, we examined sections through the hippocampus of normal young adult rats that had been administered BrdU for 2-4 weeks, followed by a chase without BrdU for 1 to 6 months. In each case the sections were stained with DAPI (blue) as well as antibodies against BrdU (green) and NeuN (red). We readily observed $BrdU^+NeuN^+$ neurons (white arrows) in the dentate gyrus of all 18 rats, consistent with prior studies (7, 18). B) A Z-series of optical sections from the same field of view shown in panel A confirmed the localization of BrdU throughout the $NeuN^+$ neuronal nuclei. No BrdU labeling was observed in control rats that did not receive BrdU (data not shown).

Figure S4: Closely apposed $BrdU^+$ glia and $BrdU^-$ neurons sometimes looked like $BrdU^+$ neurons in single optical sections, but could be distinguished upon three-dimensional analysis of a z-stack series of optical sections. The vast majority of $BrdU^+$ cells in the adult ENS were clearly negative for HuC/D (A, arrowheads). However, a small minority of $BrdU^+$ cells initially appeared to be double positive for BrdU and HuC/D (A, arrow) when only a single image was analyzed. B) A detailed, three-dimensional analysis of a z-series of 1 μm thick optical sections of these cells (B shows the same field of view as shown in panel A) revealed that the BrdU staining was present in a different cell (arrow; likely a small glial cell) adjacent to the larger HuC/D^+ nucleus (B, arrow). Note that the neuronal nucleus is still visible at the level below where the BrdU signal can be detected. This type of z-series analysis confirmed the presence of $BrdU^+HuC/D^+$ neurons in only a single rat (see Figure S7).

Figure S5: Neurogenesis was not detected in multiple regions of the adult ENS by BrdU incorporation. Whole mount staining of the myenteric plexus with DAPI (blue) and antibodies

against BrdU (green) and HuD (red) in normal young adult mice that were administered BrdU for 6 weeks followed by 6 weeks chase without BrdU. No $BrdU^+$ neurons were detected in the stomach (A), duodenum (B), ileum (C), cecum (D) and colon (E).

Figure S6: Gliogenesis was detected by BrdU incorporation in the distal ileum of adult mice with gut inflammation. Whole mount immunostaining of the myenteric plexus from the distal ileum of mice with gut inflammation from Figure 2B, 2C and 2E. While neurogenesis was not observed in these mice (Figure 2) gliogenesis was readily observed in all mice (see white arrowheads indicating representative $BrdU^+S100B^+HuD^-$ cells).

Figure S7: Clear ENS neurogenesis was observed in one adult rat that had been treated with BAC. Adult enteric neurogenesis was observed in one rat after BAC treatment. A-C) Examples of representative $BrdU^+HuC/D^+$ neurons found in the myenteric plexus of this rat (white arrow). D) Z-series images confirmed the co-localization of BrdU staining with HuC/D staining in the nuclei of these neurons (white arrow). E) Roughly 6.1% of the HuC/D^+ neurons in the injured region bordering on the gut segment treated with BAC were $BrdU^+$ and 4.7% of the HuC/D^+ neurons in a gut region 1 cm away were $BrdU^+$. Convincing $BrdU^+$ neurons were not detected in the other rats or mice listed in Table 1.

SUPPLEMENTARY TABLES

Table S1: List of primary and secondary antibodies used in this study

SUPPLEMENTARY REFERENCES

1. Kruger, G.M., Mosher, J.T., Tsai, Y.H., Yeager, K.J., Iwashita, T., Gariepy, C.E., and Morrison, S.J. 2003. Temporally distinct requirements for endothelin receptor B in the generation and migration of gut neural crest stem cells. *Neuron* 40:917-929.
2. Stemple, D.L., and Anderson, D.J. 1992. Isolation of a stem cell for neurons and glia from the mammalian neural crest. *Cell* 71:973-985.
3. Shah, N.M., Groves, A., and Anderson, D.J. 1996. Alternative neural crest cell fates are instructively promoted by TGFß superfamily members. *Cell* 85:331-343.

4. Earlam, R.J. 1971. Ganglion cell changes in experimental stenosis of the gut. *Gut* 12:393-398.
5. Brehmer, A., Gobel, D., Frieser, M., Graf, M., Radespiel-Troger, M., and Neuhuber, W. 2000. Experimental hypertrophy of myenteric neurones in the pig: a morphometric study. *Neurogastroenterol Motil* 12:155-162.
6. Bush, T.G., Savidge, T.C., Freeman, T.C., Cox, H.J., Campbell, E.A., Mucke, L., Johnson, M.H., and Sofroniew, M.V. 1998. Fulminant jejuno-ileitis following ablation of enteric glia in adult transgenic mice. *Cell* 93:189-201.
7. Chen, G.Y., Shaw, M.H., Redondo, G., and Nunez, G. 2008. The innate immune receptor Nod1 protects the intestine from inflammation-induced tumorigenesis. *Cancer Res* 68:10060-10067.
8. Martin, F., Penet, M.F., Malergue, F., Lepidi, H., Dessein, A., Galland, F., de Reggi, M., Naquet, P., and Gharib, B. 2004. Vanin-1(-/-) mice show decreased NSAID- and Schistosoma-induced intestinal inflammation associated with higher glutathione stores. *J Clin Invest* 113:591-597.
9. Logsdon, L.K., and Mecsas, J. 2003. Requirement of the Yersinia pseudotuberculosis effectors YopH and YopE in colonization and persistence in intestinal and lymph tissues. *Infect Immun* 71:4595-4607.
10. Borenshtein, D., Nambiar, P.R., Groff, E.B., Fox, J.G., and Schauer, D.B. 2007. Development of fatal colitis in FVB mice infected with Citrobacter rodentium. *Infect Immun* 75:3271-3281.
11. Kiel, M.J., Yilmaz, O.H., Iwashita, T., Terhorst, C., and Morrison, S.J. 2005. SLAM Family Receptors Distinguish Hematopoietic Stem and Progenitor Cells and Reveal Endothelial Niches for Stem Cells. *Cell* 121:1109-1121.
12. van Praag, H., Kempermann, G., and Gage, F.H. 1999. Running increases cell proliferation and neurogenesis in the adult mouse dentate gyrus. *Nature Neuroscience* 2:266-270.
13. Srinivasan, S., Stevens, M., and Wiley, J.W. 2000. Diabetic peripheral neuropathy - evidence for apoptosis and associated mitochondrial dysfunctions. *Diabetes* 49:1932-1938.
14. Kuhn, H.G., Dickinson-Anson, H., and Gage, F.H. 1996. Neurogenesis in the dentate gyrus of the adult rat: age-related decrease of neuronal progenitor proliferation. *Journal of Neuroscience* 16:2027-2033.

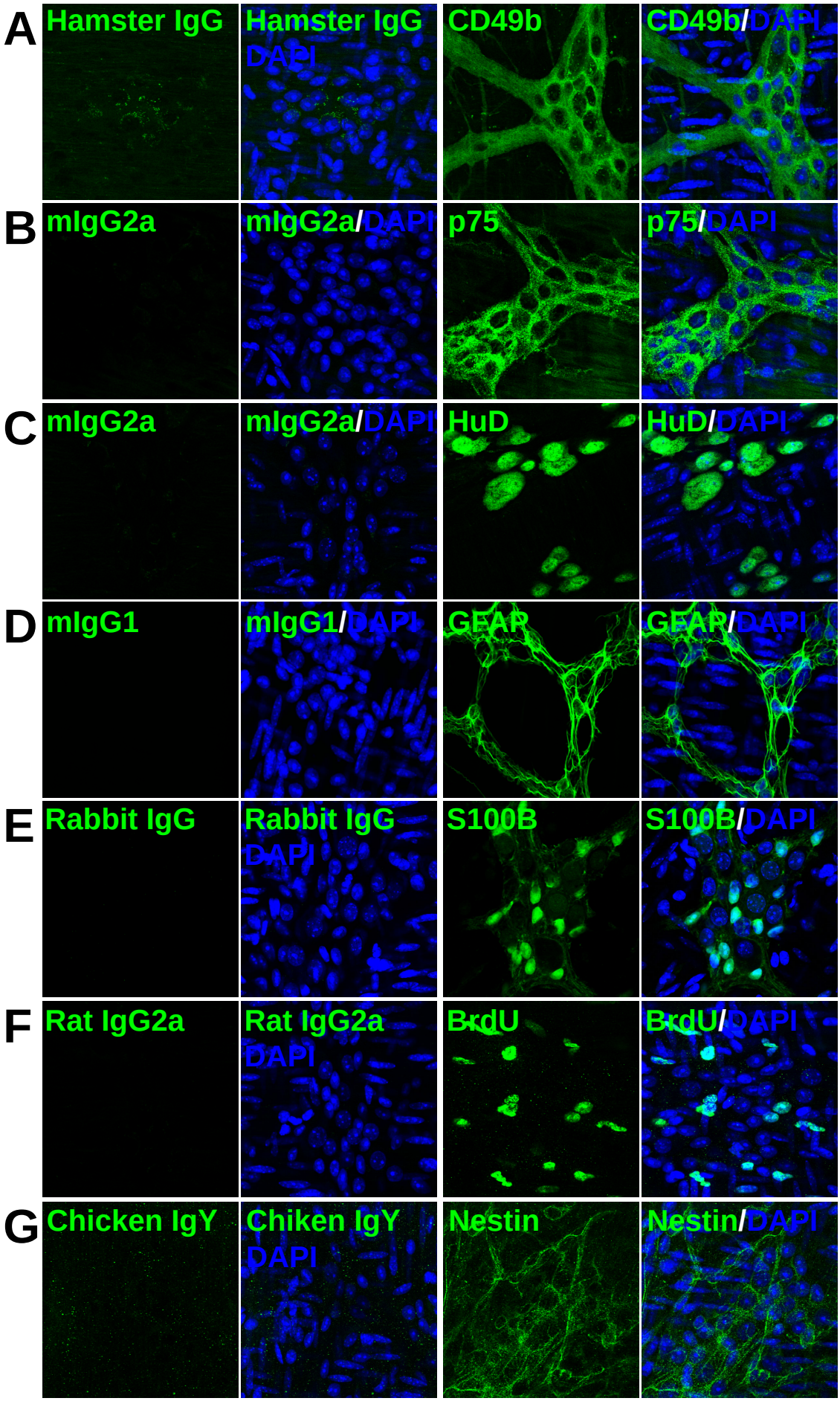

Figure S1: The specificity of primary antibody staining. A-G) To confirm the specificity of all primary antibody staining, we stained adjacent gut tissue with appropriate isotype control immunoglobulins, side-by-side with each primary antibody. In all cases, specific staining was observed with the primary antibodies, but not with isotype controls.

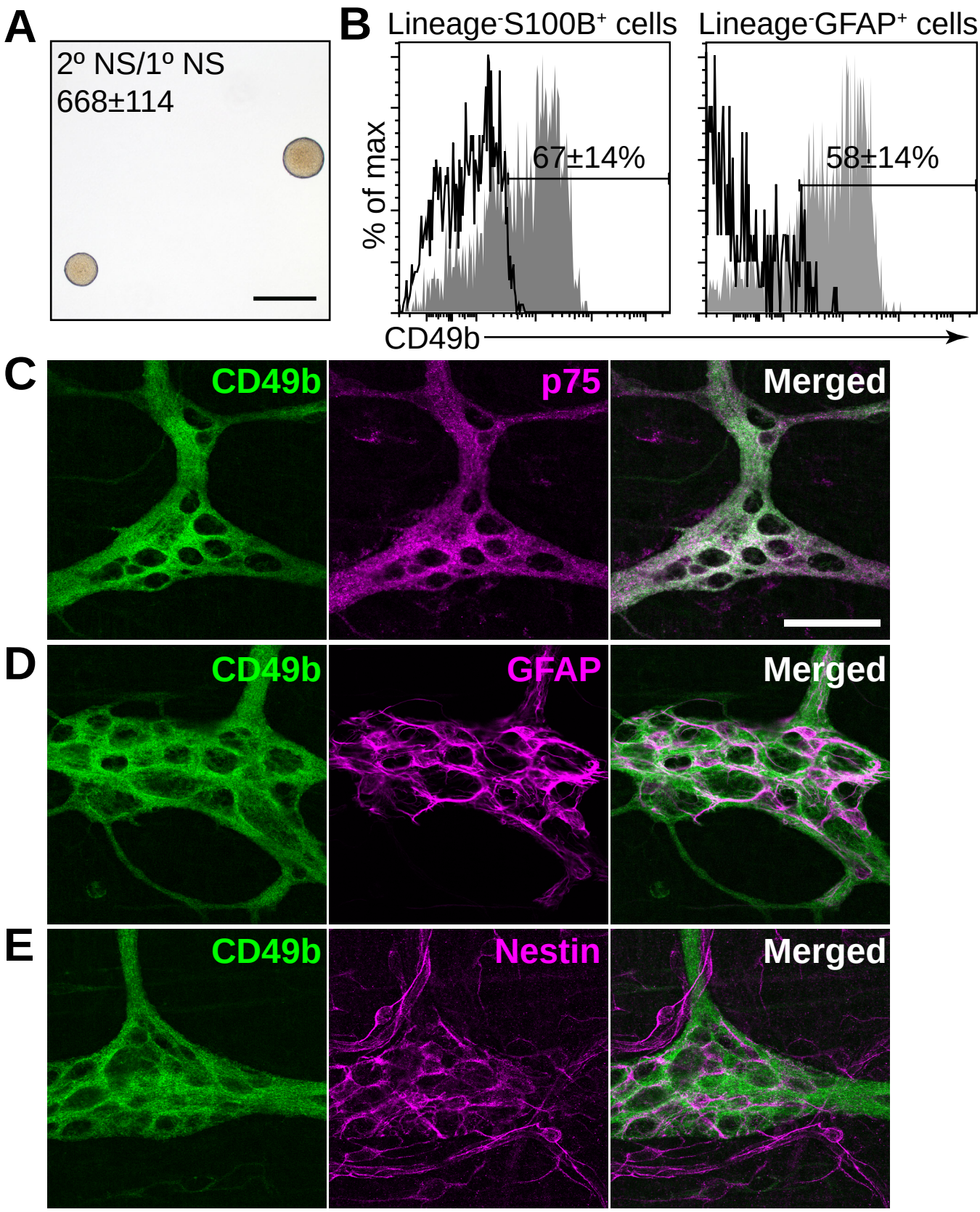

Figure S2: Most adult mouse enteric glia express CD49b. A) A representative image of secondary neurospheres derived from a single, multipotent primary neurosphere. All multipotent primary neurospheres were capable of generating secondary neurospheres. On average, each primary neurosphere generated 668±114 multipotent secondary neurospheres. B) Flow-cytometric analysis of fixed adult Lineage$^-$S100B$^+$ and Lineage$^-$GFAP$^+$ gut cells stained with isotype control antibody (open histograms) or anti-CD49b antibody (grey shaded histograms). Most Lineage$^-$S100B$^+$ and Lineage$^-$GFAP$^+$ cells were CD49b$^+$. C-E) Representative whole mount immunofluorescence staining showing CD49b staining co-localized with p75, GFAP and Nestin staining throughout adult myenteric ganglia, in a pattern consistent with enteric glia.

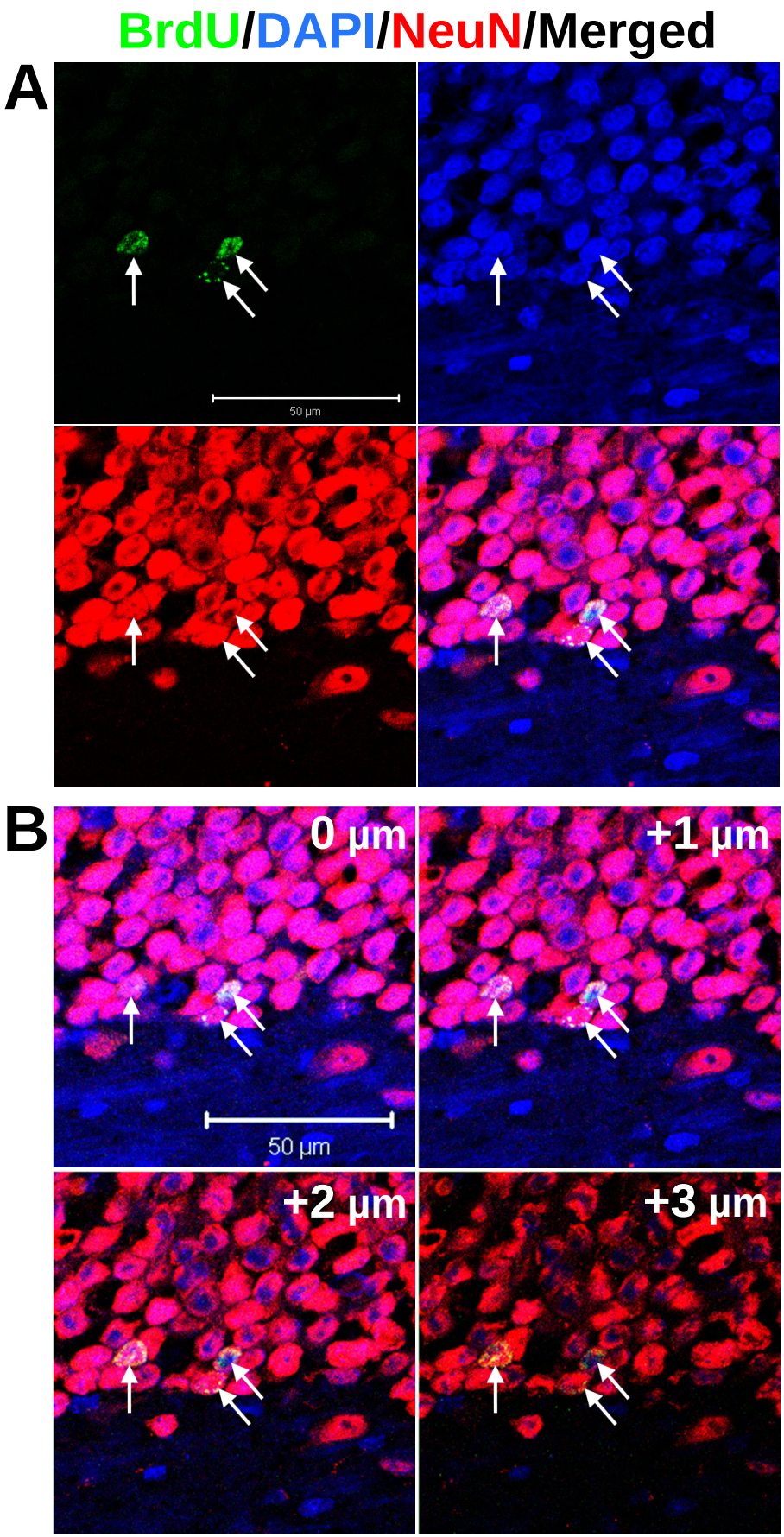

Figure S3: Neurogenesis was readily detected by BrdU incorporation in the adult dentate gyrus of all rats examined. A) As a positive control for adult neurogenesis, we examined sections through the hippocampus of normal young adult rats that had been administered BrdU for 2-4 weeks, followed by a chase without BrdU for 1 to 6 months. In each case the sections were stained with DAPI (blue) as well as antibodies against BrdU (green) and NeuN (red). We readily observed $BrdU^{+}NeuN^{+}$ neurons (white arrows) in the dentate gyrus of all 18 rats, consistent with prior studies (7, 18). B) A Z-series of optical sections from the same field of view shown in panel A confirmed the localization of BrdU throughout the $NeuN^{+}$ neuronal nuclei. No BrdU labeling was observed in control rats that did not receive BrdU (data not shown).

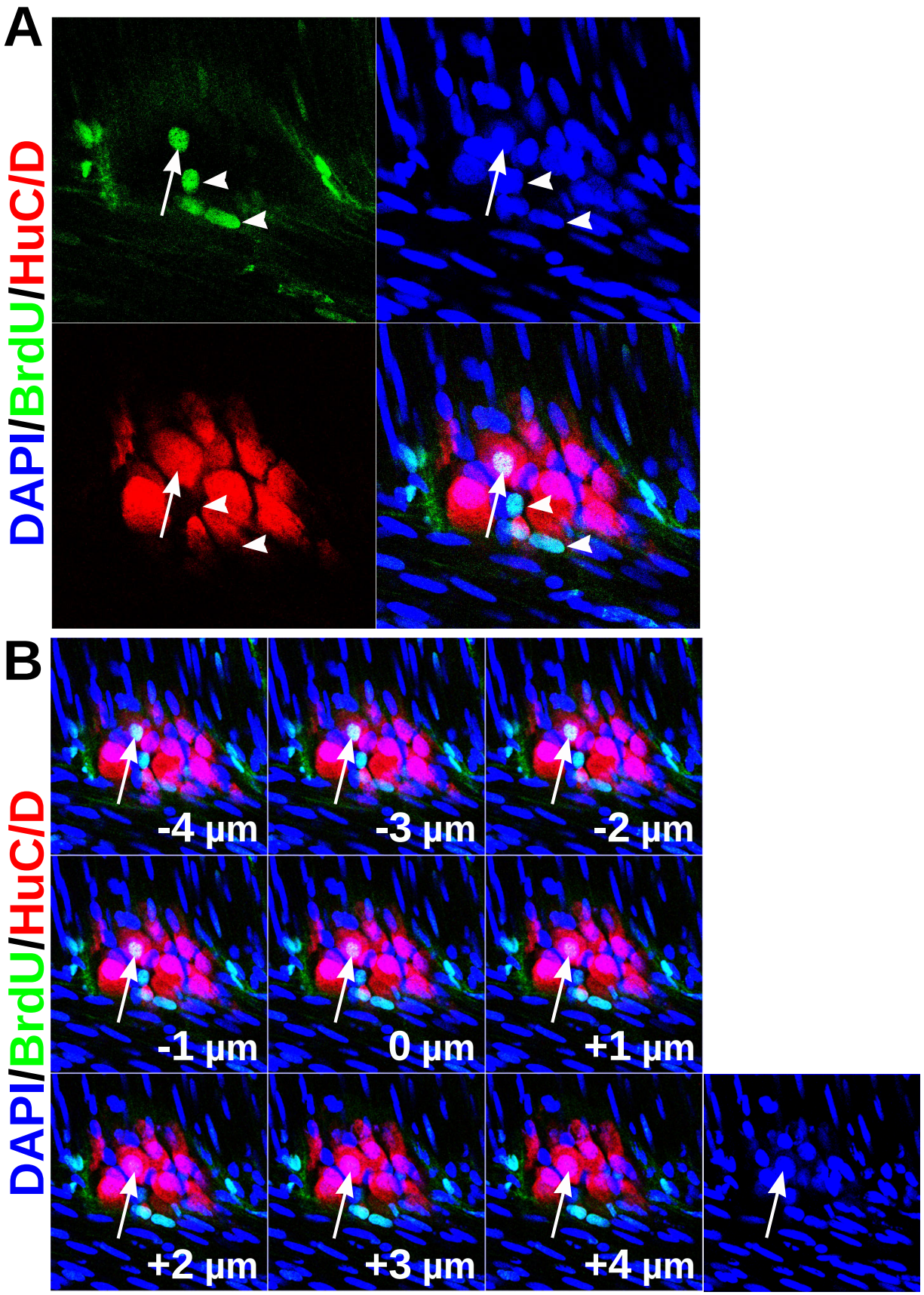

Figure S4: Closely apposed BrdU⁺ glia and BrdU⁻ neurons sometimes looked like BrdU⁺ neurons in single optical sections, but could be distinguished upon three-dimensional analysis of a z-stack series of optical sections. The vast majority of BrdU⁺ cells in the adult ENS were clearly negative for HuC/D (A, arrowheads). However, a small minority of BrdU⁺ cells initially appeared to be double positive for BrdU and HuC/D (A, arrow) when only a single image was analyzed. B) A detailed, three-dimensional analysis of a z-series of 1 µm thick optical sections of these cells (B shows the same field of view as shown in panel A) revealed that the BrdU staining was present in a different cell (arrow; likely a small glial cell) adjacent to the larger HuC/D⁺ nucleus (B, arrow). Note that the neuronal nucleus is still visible at the level below where the BrdU signal can be detected. This type of z-series analysis confirmed the presence of BrdU⁺HuC/D⁺ neurons in only a single rat (see Figure S7).

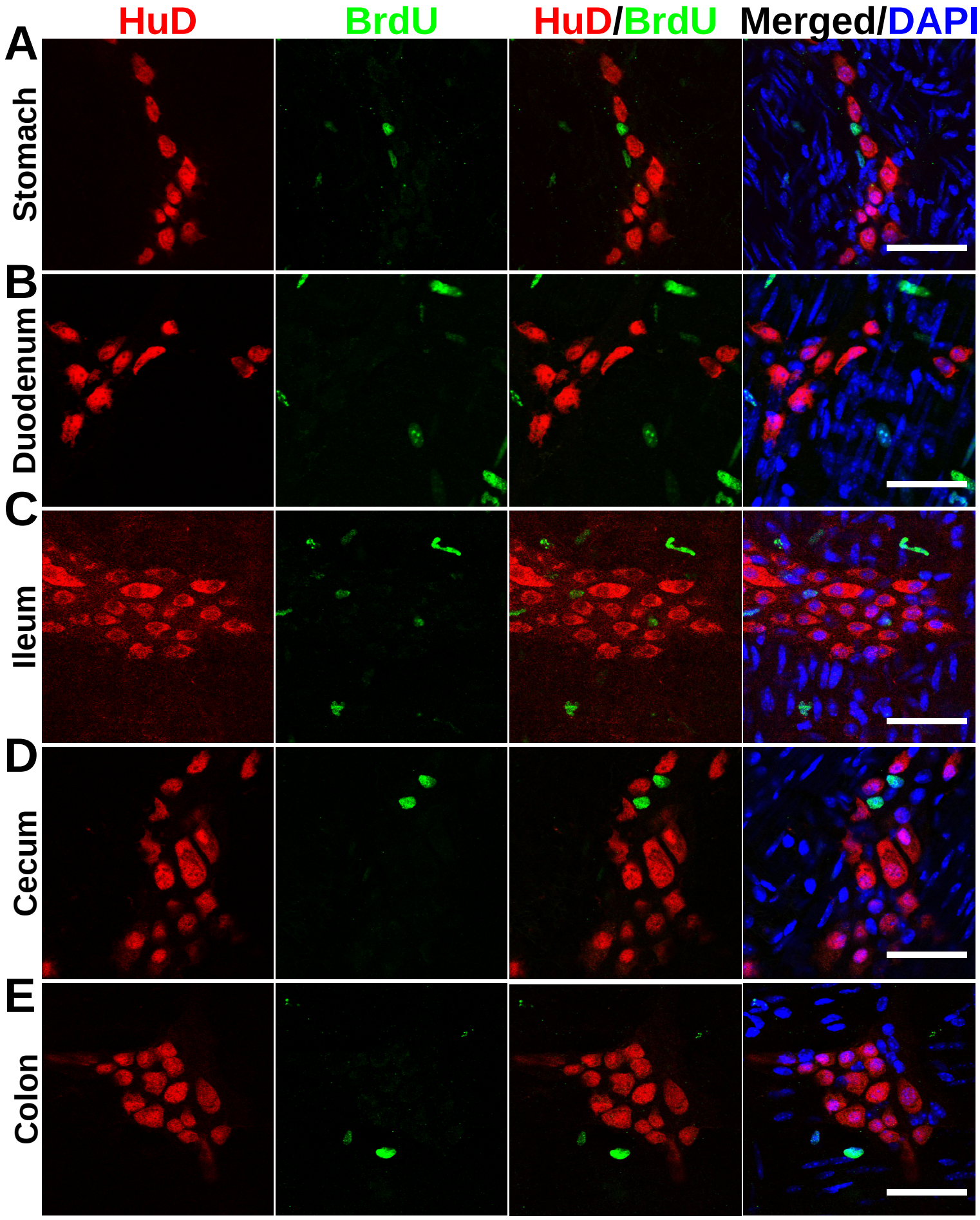

Figure S5: Neurogenesis was not detected in multiple regions of the adult ENS by BrdU incorporation. Whole mount staining of the myenteric plexus with DAPI (blue) and antibodies against BrdU (green) and HuD (red) in normal young adult mice that were administered BrdU for 6 weeks followed by 6 weeks chase without BrdU. No $BrdU^+$ neurons were detected in the stomach (A), duodenum (B), ileum (C), cecum (D) and colon (E).

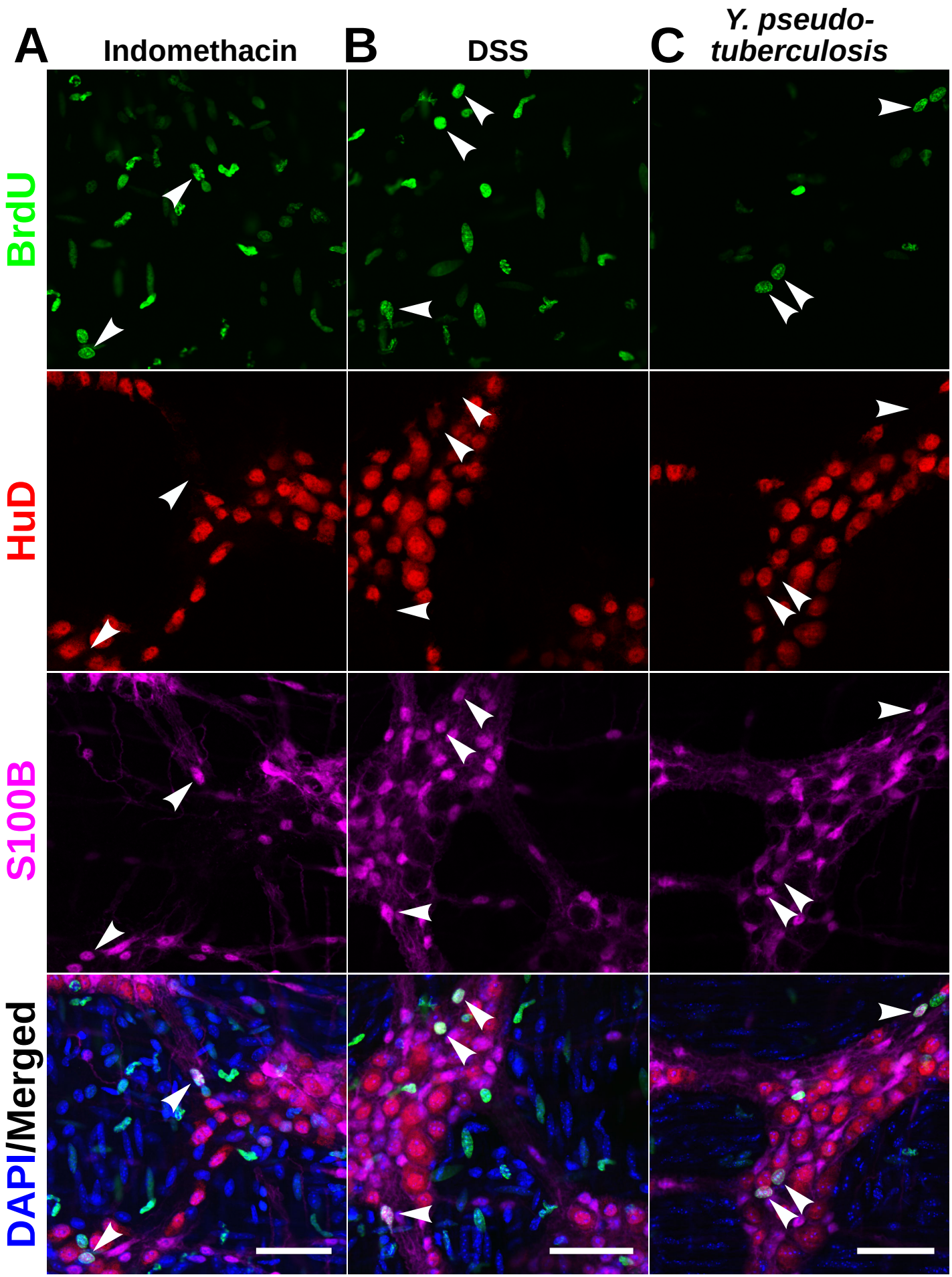

Figure S6: Gliogenesis was detected by BrdU incorporation in the distal ileum of adult mice with gut inflammation. Whole mount immunostaining of the myenteric plexus from the distal ileum of mice with gut inflammation from Figure 2B, 2C and 2E. While neurogenesis was not observed in these mice (Figure 2) gliogenesis was readily observed in all mice (see white arrowheads indicating representative $BrdU^{+}S100B^{+}HuD^{-}$ cells).

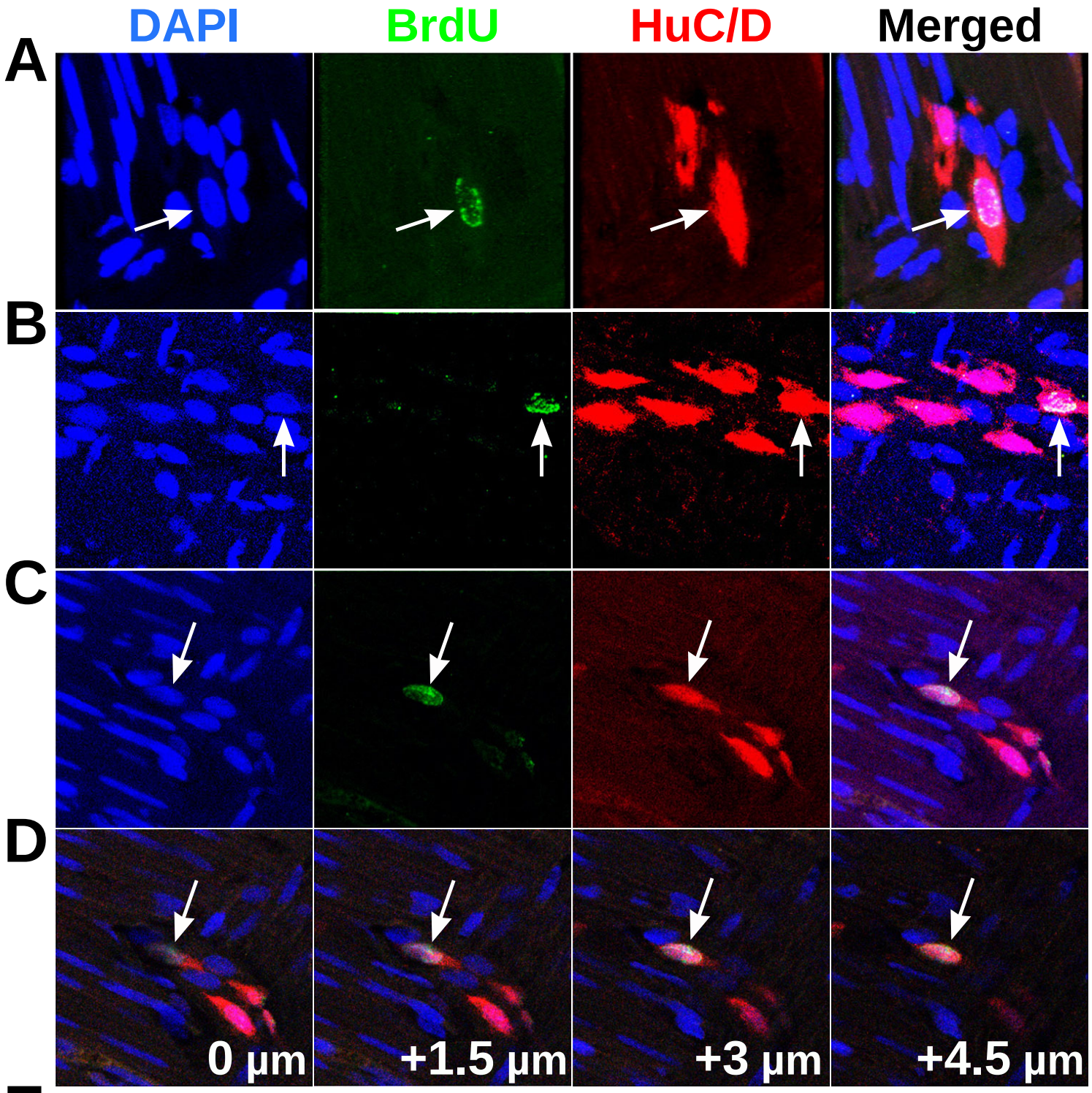

E

	BrdU+ HuC/D+	BrdU- HuC/D+	Total HuC/D+	% Neurogenesis
Injured	44	674	718	6.13
1 cm away	23	472	495	4.65

Figure S7: Clear ENS neurogenesis was observed in one adult rat that had been treated with BAC. Adult enteric neurogenesis was observed in one rat after BAC treatment. A-C) Examples of representative $BrdU^{+}HuC/D^{+}$ neurons found in the myenteric plexus of this rat (white arrow). D) Z-series images confirmed the co-localization of BrdU staining with HuC/D staining in the nuclei of these neurons (white arrow). E) Roughly 6.1% of the HuC/D^{+} neurons in the injured region bordering on the gut segment treated with BAC were $BrdU^{+}$ and 4.7% of the HuC/D^{+} neurons in a gut region 1 cm away were $BrdU^{+}$. Convincing $BrdU^{+}$ neurons were not detected in the other rats or mice listed in Table 1.

Table S1: List of primary and secondary antibodies used in this study. IF indicates immunofluorescence staining; FC indicates flow-cytometry. *, HuD and HuC/D antibodies exhibit overlapping staining in the adult ENS and label all enteric neurons.

A Primary antibodies

Antigen	Host species	Type	Clone	Conjugates	Dilution	Source
CD49b	hamster IgG2	Monoclonal	Ha1/29	FITC, Alexafluor 488	1:200 (FC, IF)	Biolegend
CD49b	rat IgM	Monoclonal	DX5	Biotin	1:200 (FC)	eBioscience
p75	mouse IgG2a	Monoclonal	MLR2	unconjugated	1:400 (FC, IF)	Millipore
BrdU	rat IgG2a	Monoclonal	BU1/75	unconjugated	1:500 (IF)	Abcam
GFP	chicken IgY	Polyclonal		unconjugated	1:5000 (IF)	Aves Labs
Cre	mouse IgG1	Monoclonal	7.23	unconjugated	1:500 (IF)	Covance, MMS-106R
Peripherin	rabbit	Polyclonal		unconjugated	1:1000 (IF)	Millipore, AB1530
Peripherin	chicken IgY	Polyclonal		unconjugated	1:1000 (IF)	Aves Labs
HuD*	mouse IgG2a	Monoclonal	E-1	unconjugated	1:200 (FC, IF)	Santa Cruz
HuC/D*	mouse IgG2b	Monoclonal	16A11	unconjugated	1:200 (IF)	Invitrogen
NeuN	mouse IgG1	Monoclonal	A60	unconjugated	1:200 (IF)	Millipore
S100B	rabbit IgG	Polyclonal		unconjugated	1:500 (IF), 1:1000 (FC)	Dako
Nestin	chicken IgY	Polyclonal		unconjugated	1:1000 (FC, IF)	Aves Labs
GFAP	mouse IgG1	Monoclonal	G-A-5	unconjugated	1:1000 (IF), 1:5000 (FC)	Sigma
αSMA	mouse IgG2a	Monoclonal	1A4	unconjugated	1:1000 (IF)	Sigma
SOX10	mouse IgG1	Monoclonal	20B7	unconjugated	1:1000 (FC)	R&D systems
CD45	rat IgG2b	Monoclonal	30-F11	APC	1:500 (FC)	eBioscience
TER119	rat IgG2b	Monoclonal	TER119	APC	1:200 (FC)	eBioscience
CD31	rat IgG2a	Monoclonal	390	APC	1:200 (FC)	eBioscience

B Secondary antibodies

Antibody	Dilution	Source
Streptavidin Alexa fluor 488	1:2000	Invitrogen
goat-anti-mouse IgG2a Alexa fluor 488	1:1000	Invitrogen
goat-anti-mouse IgG2a Alexa fluor 555	1:1000	Invitrogen
goat-anti-mouse IgG2a Alexa fluor 594	1:1000	Invitrogen
goat-anti-rabbit IgG Alexa fluor 647	1:1000	Invitrogen
goat-anti-mouse IgG1 Alexa fluor 555	1:1000	Invitrogen
goat-anti-rat IgG Alexa fluor 488	1:1000	Invitrogen
goat-anti-chicken IgY Alexa fluor 488	1:1000	Invitrogen
goat-anti-mouse IgG1 R-Phycoerythrin	1:500	Jackson ImmunoResearch
goat-anti-rabbit IgG R-Phycoerythrin	1:500	Jackson ImmunoResearch
goat-anti-chicken IgY fluorescein	1:500	Jackson ImmunoResearch